Numerical Analysis on Iron Loss and PM Loss of Permanent Magnet Synchronous Motor Considering the Carrier Harmonics

Dongsu Lee[1], Yong-Jae Kim[2], and Sang-Yong Jung[1]*

[1]*School of Electronic and Electrical Engineering, Sungkyunkwan University, Suwon 440-746, Korea*
[2]*Department of Electrical Engineering, Chosun University, Gwangju 501-759, Korea*

In this paper, the influence of inverter switching harmonics on iron loss and PM loss of Permanent Magnet Synchronous Motor (PMSM) is numerically investigated by Finite Element Method (FEM). In particular, non-linear FEM is applied for a multi-layered PM Synchronous Motors (PMSMs), Interior buried PMSM (IPMSM) and PM assisted Synchronous Reluctance Motor (PMa-SynRM), which are adoptively designed and compared for Electric Vehicle (EV) propulsion. In particular, iron loss and PM eddy-current loss under the real current waveform including the carrier harmonics from inverter switching are numerically analyzed with non-linear FEM by considering the skewed stator structure employed for minimizing spatial harmonics.

Keywords : IPMSM, PMa-SynRM, carrier harmonics, iron loss, PM loss, FEM

1. Introduction

IPMSM employing rare-earth PM has been known for an attractive candidate for EV propulsion, while PMa-SynRM employing ferrite magnet is being recognized as an alternative solution corresponding to the increased demand for non-rare-earth PMs [1-3]. In particular, the PMa-SynRM has outstanding superiorities, such as a mechanically robust rotor structure, low manufacturing costs by adopting ferrite magnets, and the relatively higher power density from outstanding flux weakening controll-ability covering higher speed [4-6].

In case of inverter driven PMSM, the carrier harmonics with switching frequency in the input current can give rise to significant iron losses and PM eddy current losses, which lead to degradation of the efficiency and the irrever-sible thermal demagnetization of PM due to the harmonic eddy currents [7].

In this paper, influence of inverter switching harmonics on iron losses and PM eddy-current losses in a multi-layered PMSM is numerically investigated by FEM [8].

*Corresponding author: Tel: +82-31-299-4952
Fax: +82-31-290-7231, e-mail: syjung@ece.skku.ac.kr

Specifically, the nonlinear FEM is applied to IPMSM and PMa-SynRM, which are purposely designed for the EV propulsion. Firstly, spatial harmonics of PMSM is numeri-cally featured with back-EMF and torque ripples, which should be identified with the nonlinear FEM when con-sidering magnetic saturation [9-13]. In addition, iron losses and PM eddy-current losses obtained with FEM under sinusoidal current waveform are analyzed by taking account of the skewed stator structure employed for minimizing spatial harmonics. Furthermore, the harmonics spectrum of the numerically obtained iron losses can be identified using Fast Fourier Transform (FFT). Likewise, identical methodology is applied to investigate the loss characteristics of IPMSM and PMa-SynRM under the real input currents including the carrier harmonics from inverter switching, and such results are compared with ones under the ideal current having a sinusoidal waveform [14]. In particular, current harmonics characterized with the di-stinctive carrier frequency is validated from the measured ones. Finally, the resultant efficiency considering the identi-fied iron loss and PM eddy-current loss as calculated, and compared for 80 kW IPMSM and PMa-SynRM.

2. Spatial Harmonic Analysis of PMSM with Sinusoidal Current Excitation

Table 1 shows the design specifications of the purposely

Table 1. Design specifications of IPMSM and PMa-SynRM.

Classification	IPMSM	PMa-SynRM
Size	Φ240 × L190	Φ230 × L200
Number of Poles	8	4
Number of Slots	36	36
PM Layers	2	5
PM Type	NdFeB 38MGOe (1.22 [T])	Ferrite 9G (0.44 [T])

Table 2. Comparison results of spatial harmonic analysis.

Classification	IPMSM	PMa-SynRM
Input Current	471.4 [A_{pk}]	528.0 [A_{pk}]
Current density	10.6 [A_{rms}/mm^2]	13.9 [A_{rms}/mm^2]
Average torque	213.3 [Nm]	213.4 [Nm]
Torque ripple	4.4 [%]	1.6 [%]
back-EMF (3,600 rpm)	115.2 [V_{Line_rms}]	42.5 [V_{Line_rms}]
back-EMF THD	2.2 [%]	0.7 [%]

designed IPMSM and PMa-SynRM for EV propulsion with the medium sedan class requiring the rated power of 80 kW at the speed of 3,600 rpm. IPMSM has 8-poles, 2-layers of PMs, and 36-slots. Such fractional number of slots per pole guarantees the desirable spatial harmonic features, such as the sinusoidal back-EMF waveform and the minimized the torque ripples, although not adopting the skewed structure. PMa-SynRM has 4-poles and 5-layers of PMs to maximize the magnetic saliency, and improves the manufacturing cost effectiveness by employing ferrite magnets. One slot-pitch stator skewed structure is applied to reduce Total Harmonic Distortion (THD) of back-EMF and torque ripples. The configuration of the prototypes and the magnetic flux density at the rated condition, numerically computed with FEM, are shown in Fig. 1(a) and (b), respectively.

Table 2 shows the average torque and its ripples at the sinusoidal current excitation, with no-load back-EMF and the THD for IPMSM and PMa-SynRM. Although more input current ($57.4A_{pk}$) is required for PMa-SynRM, but because of lower torque density, its torque ripples are reduced by 2.8% from IPMSM. In addition, no-load line-to-line back-EMF of PMa-SynRM at the base speed (3,600 rpm) is $42.5V_{Line\_rms}$, much lower than IPMSM ($115.2V_{Line\_rms}$), which has the superiority that there are no problems of huge back-EMP feedbacks during controllability breakdowns at considerably high speeds. Thanks

to the skewed structure of PMa-SynRM, its back-EMF THD remains 0.7%, less than the IPMSM (2.2%).

3. Iron Loss and PM Eddy-Current Analysis of PMSM with Harmonic Current Excitation

In case of inverter-driven PMSM, it is mandatory to consider the harmonic current excitation fed with inverter PWM switching which includes carrier frequency, coupled with nonlinear FEM and spectrum analysis [2]. In this paper, the real current having the switching frequency of 8 kHz is measured in advance and forwarded to the time-stepping numerical analysis. For reference, the ferromagnetic material of electrical core steel is S08 grade and its single sheet thickness is 0.35 mm (POSCO, Ltd).

Comparison results of individual loss at 80 kW are summarized in Table 3, where PMa-SynRM has the large copper losses due to the larger input currents. Nevertheless, its iron losses and PM eddy-current losses are lower than IPMSM model. Notably, PM eddy-current losses occurred inside ferrite magnets are infinitesimal on account of the strong electrical resistances of ferrite magnet itself, which can be regarded as another attractive perspective of PMa-SynRM [13]. Superior advantage of iron losses and PM eddy-current losses of PMa-SynRM manifests higher
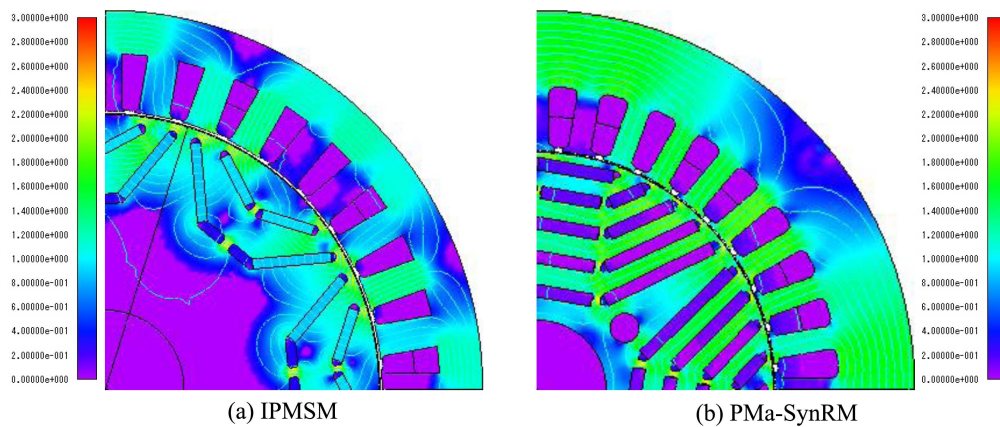

(a) IPMSM

(b) PMa-SynRM

Fig. 1. (Color online) The magnetic flux density of IPMSM and PMa-SynRM (80 kW, 3600 rpm).

Table 3. Comparison results of loss and efficiency under sinusoidal current excitation.

Classification		IPMSM	PMa-SynRM
Copper loss		1.55 [kW]	2.17 [kW]
Iron loss	Rotor	0.14 [kW]	0.12 [kW]
	Stator	0.66 [kW]	0.46 [kW]
PM Eddy-Current Loss		0.74 [kW]	-
Total Loss		3.09 [kW]	2.75 [kW]
Total Efficiency		96.3 [%]	96.7 [%]

Table 4. Comparison results of loss and efficiency under harmonic current excitation.

Classification		IPMSM	PMa-SynRM
Copper loss		1.77 [kW]	2.48 [kW]
Iron loss	Rotor	0.42 [kW]	0.17 [kW]
	Stator	1.23 [kW]	0.65 [kW]
PM Eddy-Current Loss		1.31 [kW]	-
Total Loss		4.73 [kW]	3.30 [kW]
Total Efficiency		94.4 [%]	96.0 [%]
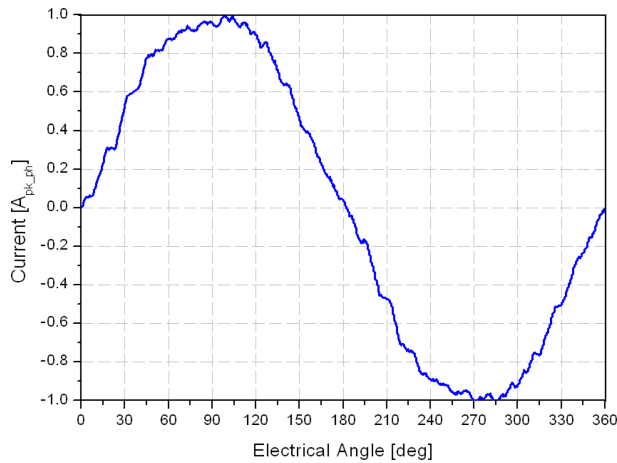
Fig. 2. (Color online) Controlled current waveform with time-harmonics (THD: 3.4%).
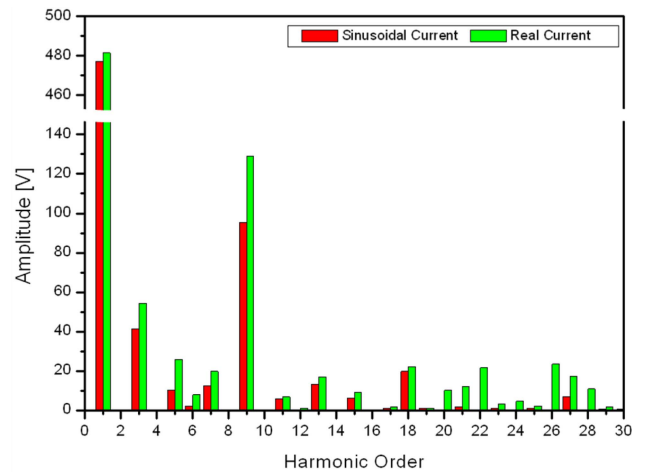
Fig. 4. (Color online) FFT analysis results of iron losses for IPMSM according to current excitation.

efficiency (96.7%) than IPMSM by 0.4%.

As mentioned previously, the real input current is measured in advance from the experiments controlled by inverter with switching frequency 8 kHz. Controlled current waveform with time-harmonics is shown in Fig. 2, and its FFT results decomposed into n-th order harmonics are shown in Fig. 3, whereby THD is 3.4%, and the 5th, the 22nd, the 26th harmonics components occupy mainly. Subsequently, this real current is employed to nonlinear
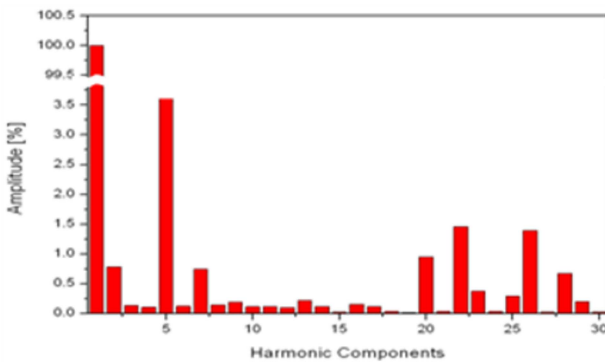
numerical analysis with time-stepping FEM for computing iron losses and PM eddy-current losses, such results are summarized in Table 4. In particular, copper loss is increased from the sinusoidal current excitation on account of the compensated larger current to maintain the average torque, and iron loss is dramatically increased mainly due
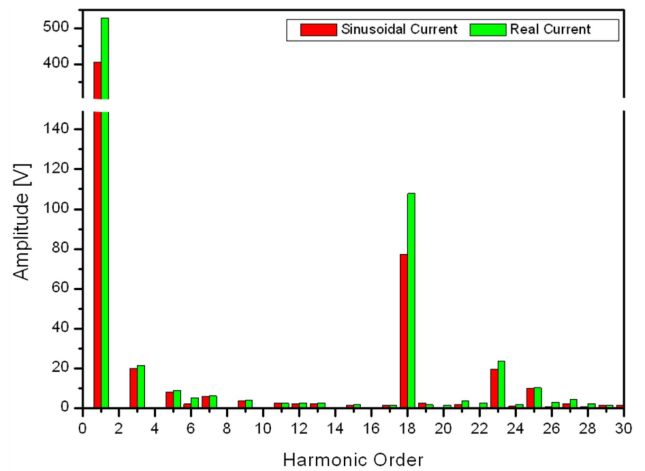

Fig. 3. (Color online) The harmonics spectrum of input current with carrier harmonics.

Fig. 5. (Color online) FFT analysis of iron losses for PMa-SynRM according to current excitation.

to the time-harmonic influences of the real current. In addition, it is obvious that PM eddy-current loss is more significant for IPMSM than PMa-SynRM with the harmonic current excitation. Thus, total loss differences between IPMSM and PMa-SynRM becomes more distinguished, and gives birth to efficiency discrepancy after all.

Meanwhile, Figs. 4 and Fig. 5 show the harmonics spectrum of iron losses for IPMSM and PMa-SynRM, respectively, obtained by FFT coupled with nonlinear FEM. Thus, it is shown that the iron loss of the real current is more significant than the sinusoidal current throughout the harmonics order, while IPMSM generates the 9th harmonic and PMa-SynRM generates the 18th harmonic outstandingly, which resulted from the different number of poles.

4. Conclusion

This paper has investigated iron losses and PM eddy-current losses numerically with nonlinear FEM, and compared for IPMSM and PMa-SynRM. Furthermore, the real current with the carrier harmonics is employed and compared with the sinusoidal current excitation. It is shown that the harmonic currents including carrier harmonics give severe influence on iron losses and PM eddy-current losses; and, it is more significant to IPMSM, whereas the PMa-SynRM has the superior tolerance against time-harmonic influence.

Acknowledgment

References

[1] Sung-Il Kim, Geun-Ho, Jung-Pyo Hong, and Tae-Uk Jung, IEEE Trans. Magn. **44**, 1590 (2008).

[2] Seungho Lee, Yu-Seok Jeon, Yong-Jae Kim, and Sang-Yong Jung, IEEE Trans. Ind. Electron. **58**, 3806 (2011).

[3] G. Pellegrino, A. Vagati, P. Guglielmi, and B. Boazzo, IEEE Trans. Ind. Electron. **59**, 3803 (2012).

[4] Kwang-Soo Kim, Seung-Joo Kim, Dong-Woo Kang, Sung-Chul Go, Yon-Do Chun, and J. Lee, IEEE Trans. Magn. **45**, 4660 (2007).

[5] M. Barcaro, N. Bianchi, and F. Magnussen, IEEE Trans. Ind. Electron. **59**, 2495 (2012).

[6] Jeihoon Baek, Sangshin Kwak, and Hamid A. Toliyat, J. Magnetics **18**, 65 (2013).

[7] Katsumi Yamazaki and Shin Jiro Watarim, IEEE Trans, Magn. **41**, 3285 (2005).

[8] M. Markovic, and Y. Perriard, Electrical Machines and Systems (ICEMS) Conf. (2008) pp. 309-313.

[9] Geun-Ho Lee, Sung-Il Kim, Jung-Pyo Hong, and Ji-Hyung Bahn, IEEE Trans. Magn. **44**, 1582 (2008).

[10] G. Y. Sizov, D. M. Ionel, and N. A. O. Demerdash, IEEE Trans. Ind. Electron. **59**, 2403 (2012).

[11] Young-Kyoun Kim, J. Magnetics **17**, 280 (2012).

[12] Won-Ho Kim, Ik-Sang Jang, Ki-Doek Lee, Jong-Bin Im, Chang-Sung Jin, Dae-Hyun Koo, and Ju Lee, J. Magnetics **16**, 71 (2011).

[13] Jinwoo Lim, Yong Jae Kim, and Sang-Yong Jung, J. Magnetics **16**, 417 (2011).

[14] Yun-Ho Jeong, Kwangdeok Kim, Yong-Jae Kim, Byung-Sup Park, and Sang-Yong Jung, Electrical Machines (ICEM), 2012 XXth International Conf. (2012) pp. 164-170.